TROP2 Is Associated with Primary Resistance to Immune Checkpoint Inhibition in Patients with Advanced Non–Small Cell Lung Cancer

Alban Bessede[1], Florent Peyraud[2,3,4], Benjamin Besse[5], Sophie Cousin[2], Mathilde Cabart[2], François Chomy[2], Christophe Rey[1], Oren Lara[1], Ophélie Odin[1], Imane Nafia[1], Lucile Vanhersecke[2], Fabrice Barlesi[5], Jean-Philippe Guégan[1], and Antoine Italiano[2,3,4]

ABSTRACT

Purpose: Mechanisms of primary resistance to inhibitors of the programmed cell death-1 (PD-1)/programmed death-ligand 1 (PD-L1) signaling axis in non–small cell lung cancer (NSCLC) are still poorly understood. While some studies suggest the involvement of trophoblast cell surface antigen 2 (TROP2) in modulating tumor cell resistance to therapeutic drugs, its specific role in the context of PD-1/PD-L1 axis blockade is not definitively established.

Experimental Design: We performed high-throughput analysis of transcriptomic data from 891 NSCLC tumors from patients treated with either the PD-L1 inhibitor atezolizumab or chemotherapy in two large randomized clinical trials. To confirm our results at the protein level, we complemented this transcriptional approach by performing a multiplex immunofluorescence analysis of tumor tissue samples as well as a proteomic profiling of plasma.

Results: We observed a significant association of TROP2 overexpression with worse progression-free survival and overall survival on PD-L1 blockade, independent of other prognostic factors. Importantly, we found increased TROP2 expression to be predictive of survival in patients treated with atezolizumab but not chemotherapy. TROP2 overexpression was associated with decreased T-cell infiltration. We confirmed these results at the proteomic level both on tumor tissue and in plasma.

Conclusions: Our results suggest an important contribution of TROP2 expression to the primary resistance to PD-L1 blockade in NSCLC. TROP2-biomarker–based strategy may be relevant in selecting patients with NSCLC who are more likely to benefit from a combination of immunotherapy and an anti-TROP2 agent.

Introduction

Despite numerous efforts to decrease tobacco consumption, lung cancer remains the leading cause of cancer-related death in Western countries. A significant portion of patients (80%) diagnosed with non–small cell lung cancer (NSCLC) have already progressed to an advanced stage. The advent of mAbs targeting programmed cell death-1 (PD-1) or its ligand, programmed death-ligand 1 (PD-L1), has brought about a revolutionary shift in the management of advanced NSCLC, with several studies demonstrating notable improvements in objective response rate, progression-free survival (PFS), and overall survival (OS) (1). However, most patients with advanced NSCLC exhibit primary resistance to PD-1/PD-L1 blockade, and the underlying mechanisms responsible for this phenomenon are still poorly understood (2).

Trophoblast cell surface antigen 2 (TROP2), also known as tumor-associated calcium signal transducer 2, is a crucial 36-kDa single-pass transmembrane protein that exhibits high expression levels in various epithelial cancers. Although the precise physiologic role of TROP2 is still being investigated, research has revealed its involvement in multiple intracellular signaling pathways such as MAPK and PI3K/AKT. These pathways are closely associated with critical processes like cell proliferation, migration, and invasion, which are key factors in cancer progression (3–5).

TROP2 expression has been found in nearly all lung cancer cells, although the extent of its expression varies, and high expression levels are only observed in a specific subset of cases (6–7). Preclinical data have suggested that TROP2 surface expression in lung cancer cells may affect the functions of cancer cell–reactive T cells by inducing apoptosis of $CD8^+$ T cells (8).

To investigate the impact of TROP2 expression on the treatment outcomes of patients with NSCLC undergoing immunotherapy, we initially analyzed the largest NSCLC gene expression dataset available worldwide. This dataset comprises whole-transcriptome profiles of 891 pretreatment tumors from two randomized studies, the POPLAR study (phase II; ref. 9) and the OAK study (phase III; ref. 10), which assessed the safety and efficacy of atezolizumab versus the cytotoxic agent docetaxel as a second-line treatment of NSCLC. To validate our findings at the protein level, we complemented this transcriptomic analysis with multiplex immunohistofluorescence (mIHF) on tumor tissue and with proteomic profiling of plasma.

Materials and Methods

Patient population

Gene expression data were collected from patients included in the open-label, randomized phase II POPLAR (NCT01903993) and phase III OAK trials (NCT02008227), which evaluated atezolizumab versus docetaxel in patients with NSCLC who progressed following

[1]Explicyte, Bordeaux, France. [2]Department of Medicine, Institut Bergonié, Bordeaux, France. [3]Faculty of Medicine, Bordeaux, France. [4]DITEP, Gustave Roussy, Villejuif, France. [5]Department of Medicine, Gustave Roussy, Villejuif, France.

Corresponding Author: Antoine Italiano, Institut Bergonié, Department of Medicine, 229 cours de l'Argonne, Bordeaux 33000, France. E-mail: a.italiano@bordeaux.unicancer.fr

Clin Cancer Res 2024;30:779–85

doi: 10.1158/1078-0432.CCR-23-2566

Translational Relevance

A significant subgroup of non–small cell lung cancer (NSCLC) cases fails to respond to immune checkpoint inhibitors (ICI). Trophoblast cell surface antigen 2 (TROP2) is a transmembrane glycoprotein that is overexpressed in NSCLC and represents a target for antibody–drug conjugates. Overexpression of TROP2 has been shown to promote tumor cell proliferation, survival, and metastasis. We have demonstrated that TROP2 overexpression is associated with primary resistance to ICI but not to chemotherapy in patients with advanced NSCLC. These findings suggest that patients with NSCLC with TROP2-overexpressing tumors may benefit from strategy combining ICI with anti-TROP2 agents.

platinum-based chemotherapy (9, 10). Participants in both studies were administered either 1,200 mg of intravenous atezolizumab every 3 weeks until disease progression or loss of clinical benefit, or 75 mg/m^2 of intravenous docetaxel every 3 weeks until progressive disease. Results from the POPLAR and OAK trials demonstrated a noteworthy enhancement in OS with atezolizumab compared with docetaxel, regardless of PD-L1 expression. It is noteworthy that no crossover was permitted, and OS served as the primary endpoint in these trials (9, 10).

mIHF analysis and plasma proteomic profiling were performed on tumor and blood samples from patients included in an institutional molecular profiling program [Bergonie Institute Profiling (BIP) study, sponsor: Institut Bergonié, Bordeaux, France, NCT02534649]. The inclusion criteria were age ≥ 18 years, histologic confirmation of malignant tumor, unresectable and/or metastatic disease, at least one tumor evaluation by imaging after initial immunotherapy administration, and available paraffin-embedded tumor material obtained before initial immunotherapy administration.

Written informed consent was obtained from all patients. The studies were conducted in accordance with the Declaration of Helsinki and approved by the Institutional Review Board of Institut Bergonié.

The best response to treatment was evaluated according to RECIST (11). Durable clinical benefit (DCB) was defined as the proportion of patients achieving objective response or stable disease lasting ≥ 12 months. PFS was defined as the time from the start of treatment until disease progression, death, or last patient contact. OS was defined as the time from the start of treatment until death or last patient contact.

RNA sequencing data analysis

FASTQ files generated during the POPLAR (GO28753) and OAK (GO28915) clinical trials were downloaded from the European Genome-Phenome Archive (EGAC00001002120). Raw data were first processed through fastp software (v0.32.2) to remove reads containing adapters, poly-N sequences, and reads with low quality. Paired-end clean reads were mapped to the human reference genome (GRCh38 - Gencode release 39) and counted using STAR software (v2.7.10a). Differentially expressed genes were tested using the DESeq2 R package (v1.36.0), and gene signature enrichment analyses were performed using the fsgea R package (v1.22.0) with Gene Ontology–Biological Process (GO–BP) terms. Immune cell estimations were performed, and tertiary lymphoid structure (TLS) signature scores were calculated by the single-sample gene set enrichment analysis (GSEA) framework using the consensusTME R package (v0.0.1.9) with the Bindea and colleagues (12) gene set and the Hennequin and colleagues (13) gene signature, respectively. To assess the PD-L1 status for all the patients treated with atezolizumab, an optimal cut-off point was defined to classify the patients as PD-L1–high (≥ 1%) or PD-L1–low (< 1%) using the cutpointr R package (v1.1.2), and the maximize metric method was used for the patients with PD-L1 22C3 measurements. ROC curves and volcano plots were drawn using the ROCit R package (v2.1.1) and EnhancedVolcano R package (v1.14.0), respectively.

For patients enrolled in the BIP study, RNA sequencing (RNA-seq) was performed as previously described (14).

Multiplex immunofluorescence

Multiplex immunofluorescence analyses were performed on the automated Ventana Discovery XT staining platform (Ventana Medical Systems). In brief, slides of tumor tissue were deparaffinized, and antigen retrieval was performed by heat-induced epitope retrieval using standard CC1 reagent (Tris-based buffer, pH 8.0; Ventana Medical Systems). The slides were then incubated with primary antibodies against the following molecules: CD8 (C8/144B, Dako: Agilent Technologies), PanCK (AE1/AE3/PK26, Ventana), PD-L1 (QR-1, Diagomics) and TROP2 (EPR2043, Abcam).

Bound primary antibodies were detected using OmniMap horseradish peroxidase (HRP)-conjugated anti-rabbit IgG (760–4311; Ventana; Roche) or OmniMap HRP-conjugated anti-mouse IgG (760–4310; Ventana; Roche), followed by tyramide signal amplification using opal fluorophores (Opal 480, Opal 520, Opal 620, and/or Opal 690; Akoya Biosciences). The slides were counterstained with spectral 4′,6-diamidino-2-phenylindol (Akoya Biosciences), cover-slipped, and digitized using a multispectral imaging platform (PhenoImager HT, Akoya).

The multispectrally acquired images were unmixed using spectral libraries previously built from images stained for each fluorophore (monoplex) and with inForm Advanced Image Analysis software (inForm v.2.60; Akoya Biosciences). Tumor areas of each tissue slide were delineated by a pathologist using PhenoChart (Akoya Biosciences), and the annotated sections were analyzed using inForm software (v.2.6.0). Cells were segmented on the basis of DAPI and fluorescent membrane signals. Mean fluorescent marker intensities for each cell were extracted, and signal intensities were normalized using the GaussNorm function from the flowStats R package (v4.8.2). Cells were ultimately phenotyped using a thresholding method in FlowJo software (v.10.8.0; FlowJo).

Plasma proteome analysis

Proteome analysis has been carried out as previously described thanks to the Olink Proximity Extension Assay (PEA; Olink Proteomics AB, Uppsala, Sweden; ref. 15). In brief, pairs of oligonucleotide-labeled antibody probes bind to their targeted protein, and if the two probes are brought in proximity, the oligonucleotides will hybridize in a pairwise manner. The addition of a DNA polymerase leads to a proximity-dependent DNA polymerization event, generating a unique target sequence analyzed through either next-generation sequencing or real-time PCR.

Analysis of samples has been carried out using the Olink Explore 1536 library consisting of 1,472 proteins and 48 controls assays divided into four 384-plex panels focused on inflammation, oncology, cardiometabolic, and neurology proteins. Sequencing was carried out on a NovaSeq 6000 system using two S1 flow cells with 2 × 50 base read lengths. Counts of known sequences are thereafter translated into normalized protein expression (NPX) units through a quality control and normalization process developed and provided by Olink.

Data were quality controlled and normalized using an internal extension control and an inter-plate control, to adjust for intra- and inter-run variation. The final assay readout is presented in NPX values, which is an arbitrary unit on a $\log_2$-scale where a high value corresponds to a higher protein expression. All assay validation data (detection limits, intra- and inter-assay precision data, etc.) are available on the manufacturer's website (www.olink.com).

Survival and statistical analyses

The Wilcoxon and χ^2 tests were used in instances where they were deemed appropriate. For survival analyses, the log-rank test was used to compare Kaplan–Meier survival curves (survival R package v3.3.1). The Cox proportional hazards regression model was used to estimate HR and 95% confidence intervals (CI). Patients were classified as TROP2-high or TROP2-low based on an optimized threshold obtained using the maximally selected rank statistics from the maxstat R package and using PFS as the optimal outcome (survminer R package v0.4.9). Multivariable Cox proportional hazards regression models were used to compare the interdependence of distinct biomarkers for the prediction of immune checkpoint inhibitor (ICI) benefit (survivalAnalysis R package v0.3.0). All analyses were conducted using R v.4.2.1.

Availability of data and material

Raw and processed transcriptomic data and limited clinical data have been deposited at the European Genome-phenome Archive (EGA), which is hosted by the EBI and the CRG, under accession number EGA: EGAS00001005013. Additional clinical data are available via request from https://vivli.org/ourmember/roche/. The immunofluorescence datasets are not publicly available due to information that could compromise research participant consent. According to French/European regulations, any reuse of the data must be approved by the ethics committee. Each request for access to the immunofluorescence dataset (including the images) will be granted after a request is sent to the corresponding author (A. Italiano) and approval by the ethics committee.

Results

TROP2 gene expression is independently associated with unfavorable outcome in patients treated with atezolizumab but not with chemotherapy

We first investigated the impact of the *TROP2*-encoding gene (TACSTD2) expression on the PFS of patients treated with atezolizumab ($n = 405$). The clinical characteristics of these patients are summarized in Supplementary Table S1. As shown in **Fig. 1A**, the PFS of patients with high expression of *TACSTD2* was significantly lower than that of patients with low expression (median PFS, 2.5 vs. 4.1 months; $P < 0.001$). Strikingly, high *TACSTD2* expression was also associated with worse OS (median OS, 12.6 vs. 16.3 months; $P = 0.007$; **Fig. 1B**) and a lower DCB rate (15.7% vs. 26.2%; $P = 0.009$; **Fig. 1C**). None of these correlations were observed in the docetaxel arm (**Fig. 1D–F**), suggesting a predictive value of *TACSTD2* gene expression specifically for response to atezolizumab. Other factors associated with PFS and OS in patients treated with atezolizumab in the univariate analysis were histologic subtype, *CD274* gene expression, and increased TLS signatures. On multivariate analysis, high *TACSTD2* expression remained independently associated with worse PFS (Supplementary Table S2, Supplementary Fig. S1).

GO–BP enrichment analysis revealed that several immune pathways, such as the B-cell receptor and immune response–regulating pathways, were enriched in the group with low expression of *TACSTD2* (**Fig. 1G** and **H**). By using a deconvolution approach, we also found that the tumor microenvironment (TME) composition differed significantly between *TACSTD2*-high and *TACSTD2*-low tumors. *TACSTD2*-low tumors were characterized by the highest expression of genes specific to immune cell populations such as T follicular helper (Tfh) cells, T cells and cytotoxic lymphocytes and B cells (**Fig. 1I** and **J**). Analysis of an independent set of 72 NSCLC tumors, treated with ICI and incorporated into the Bergonié Institute Profiling program (BIP, NCT02534649), echoed our findings, further solidifying the association between TROP2 gene expression and poor response to ICI (Supplementary Fig. S2 and Supplementary Table S3).

TROP2 intracellular expression is associated with worse outcome in patients treated with ICI

To validate our findings at the protein level, we supplemented our transcriptional study by conducting mIHF analysis using a 5-plex color panel. This panel combined the markers PanCK, TROP2, CD8, PD-L1, and DAPI. We applied this analysis to a subset of 50 patients for whom paraffin-embedded material was available (**Fig. 2A**). The characteristics of these patients are presented in Supplementary Table S4. TROP2 is known to be cleaved in two products: the extracellular domain (ECD) and the intracellular domain (ICD; ref. 16). The ECD is shed and found only on the plasma membrane and in the cytoplasm. The ICD, which is the functionally dominant part of TROP2, is released from the membrane and accumulates in the nucleus where it promotes tumorigenesis. Although the total or membrane level of TROP2 expression was not associated with outcome (**Fig. 2B–D**), the intracellular expression was significantly associated with worse PFS (median 1.4 vs. 13.4 months; $P = 0.038$; **Fig. 2E**), OS (median 6.9 vs. 30.7 months; $P = 0.226$; **Fig. 2F**) and DCB rate (16.7% vs. 60.5%; $P = 0.008$; **Fig. 2G**).

Circulating TROP2 levels are associated with worse outcome in patients treated with ICI

To confirm the importance of TROP2 cleavage in the prediction of ICI response, we aimed to investigate the predictive value of circulating TROP2 levels in patients with NSCLC undergoing immunotherapy. To achieve this, we employed proteomics analysis using PEA technology (see Methods) on plasma samples collected from 74 patients with advanced NSCLC and enrolled prospectively in the BIP study (Supplementary Table S4). First, our findings demonstrate a significant correlation between circulating TROP2 levels and TROP2 gene expression in tumor tissue (Supplementary Fig. S2A). Interestingly, when classifying TROP2 circulating levels as high or low, we observed a significant correlation with DCB rate (17.5% vs. 52.9%; $P = 0.003$; Supplementary Fig. S2B), PFS (median 2.4 vs. 10.9 months; $P = 0.003$; Supplementary Fig. S2C), and OS (median 8.5 vs. 24.6 months; $P = 0.045$; Supplementary Fig. S2D). In addition, we conducted an in-depth analysis of the tumor's transcriptomic profile based on the peripheral TROP2 status (low vs. high; Supplementary Fig. S2E). Through GSEA, we identified the MEK signaling pathway as significantly induced in circulating TROP2-high patients. This finding strongly suggests a correlation between TROP2 cleavage and MEK activation, which is supported by existing literature evidence (ref. 17; Supplementary Fig. S2F). Moreover, our observations revealed that a high level of circulating TROP2 was associated with a reduction in gamma delta T cells and Th1 cells within the TME (Supplementary Fig. S2G).

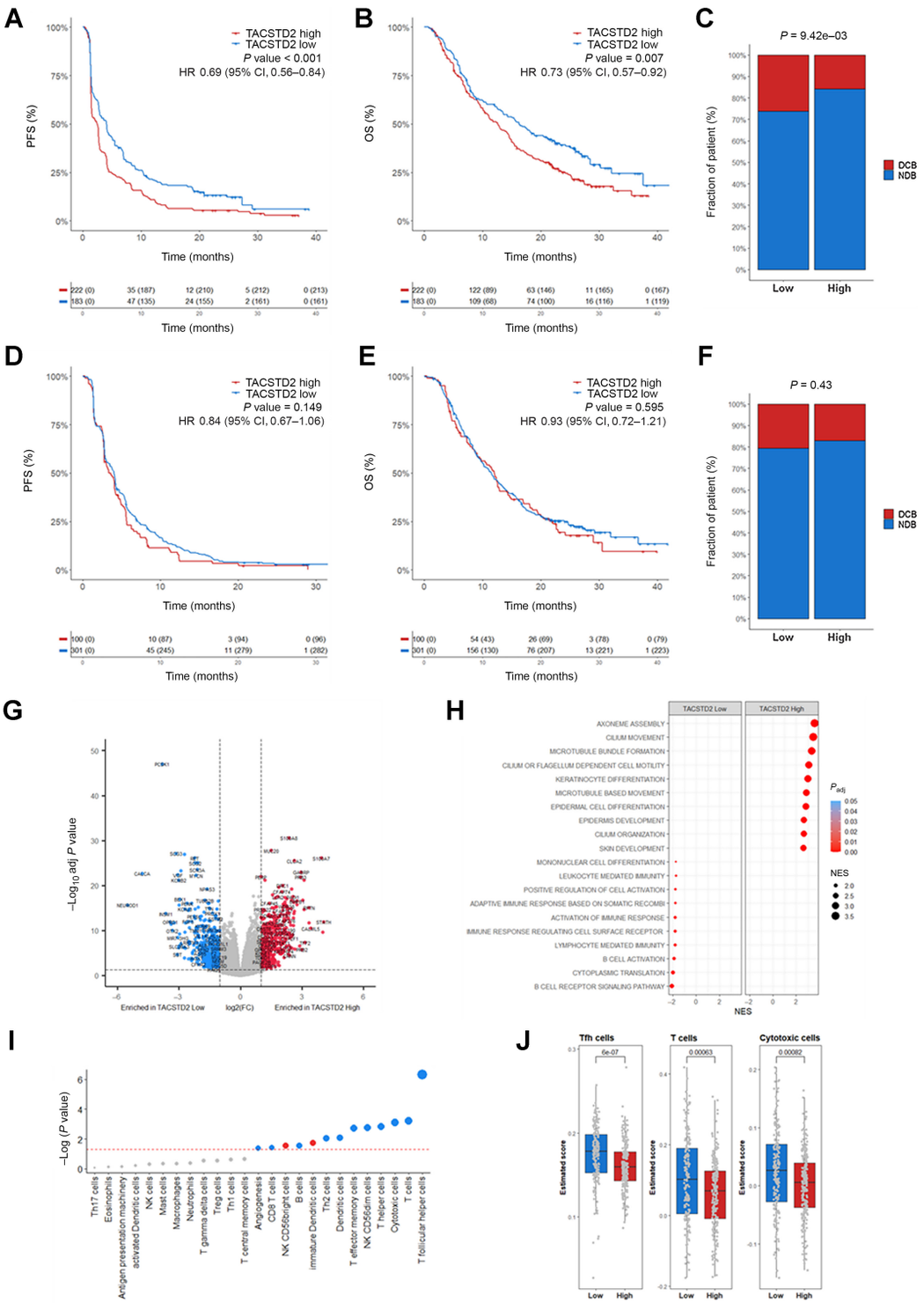

Figure 1.

High *TACSTD2* gene expression correlates with poorer response to ICI. Patients from the POPLAR and OAK studies were classified as high or low based on their baseline level of TACSTD2 gene expression as assessed by RNA-seq. Kaplan–Meier curves of the PFS (**A**–**D**) and OS (**B**–**E**) of patients treated with atezolizumab (**A** and **B**) or docetaxel (**D** and **E**). **C**–**F**, Proportion of patients treated with atezolizumab (**C**) or docetaxel (**F**) with high and low expression of TACSTD2 who experienced DCB or nondurable clinical benefit (NDB). *P* values were calculated using a χ^2 test. **G,** Volcano plot representation of the gene differentially expressed between TACSTD2-high and TACSTD2-low patients. **H,** GO analysis of the gene differentially expressed between TACSTD2-high and TACSTD2-low patients. **I,** Estimation of the immune microenvironment of patients with high and low TCASTD2 gene expression by data deconvolution using Bindea and colleagues gene sets. **J,** Histograms of the estimated score of Tfh, T cells, and cytotoxic cells in TACSTD2-high and TACSTD2-low patients. *P* values were calculated using the Wilcoxon test.

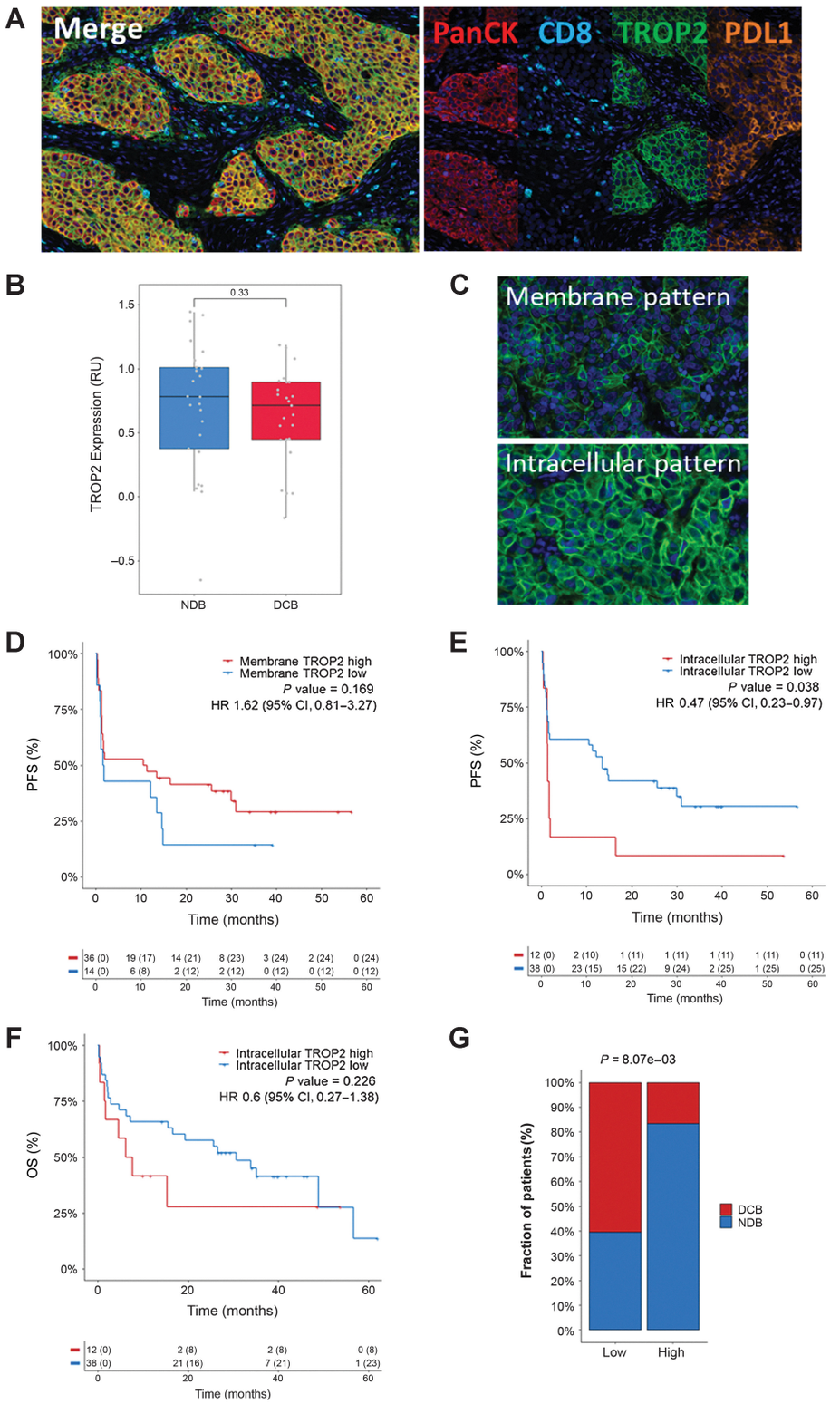

Figure 2.

TROP2 nuclear activity is associated with poor response to immunotherapy in NSCLC cancer patients. **A,** Representative image field CD8/PanCK/PD-L1/TROP2/DAPI mIHF panel on a lung adenocarcinoma section. **B,** Histogram of the level of TROP2 expression in patients treated with immunotherapy who experienced DCB or nondurable clinical benefit (NDB). *P* value was calculated using the Wilcoxon test. **C,** TROP2 expression pattern in patients with NSCLC. A clear membrane staining (top) can be distinguished from more diffuse staining (bottom), with nuclear localization. **D** and **E,** Kaplan–Meier curves of the PFS of patients stratified as high versus low membrane TROP2-positive tumors (**D**) or high versus low intracellular TROP2-positive tumors (**E**). **F,** Kaplan–Meier curves of the OS of patients with high versus low intracellular TROP2-positive tumors. **G,** Proportion of patients with high versus low intracellular TROP2-positive tumors who experienced DCB or nondurable clinical benefit (NDB). *P* value was calculated using the χ^2 test.

Discussion

Prospectively designed clinical trials are considered as the gold-standard approach for validating predictive markers. However, conducting prospective trials can be time-consuming and expensive. As an alternative, using data from previously well-conducted randomized controlled trials that compared therapies for which a marker is proposed to be predictive can offer a more feasible and timely option to test the predictive ability of a marker. In this study,

we used data from two large prospective studies that investigated the efficacy of immunotherapy (atezolizumab) versus chemotherapy (docetaxel) in patients with advanced NSCLC to examine the predictive role of TROP2 gene expression for immunotherapy efficacy. Our findings indicate that high TROP2 gene expression is associated with worse outcomes in patients with NSCLC treated with immunotherapy but not with chemotherapy. This suggests that TROP2 expression is not prognostic per se but rather predictive of immunotherapy resistance. This statement aligns with previous studies that have found no significant prognostic impact of TROP2 expression in NSCLC (6). It is also consistent with findings from The Cancer Genome Atlas (TCGA) study, showing no significant impact of TROP2 gene expression on survival in patients with resected NSCLC (TCGA data accessed at http://gepia.cancer-pku.cn/ on June 2, 2023).

Recent studies have highlighted a correlation between TROP2 expression and the TME (18). In our study, we observed that TROP2 overexpression in NSCLC was linked to decreased levels of T-cell infiltration. Although preclinical studies have indicated a potential role of TROP2 in inducing T-cell apoptosis (8), the precise mechanisms involved in the potential immunoregulatory role of TROP2 are yet to be fully understood and elucidated. Moreover, it would be interesting to explore in subsequent studies the potential role of TROP2 in mediating primary resistance to the combination of PD-1 inhibition and platinum-based chemotherapy, the current first-line standard of care. Understanding the subtleties of this interaction, especially when considering PD-L1 versus PD-1 targeting, is essential to enhance therapeutic strategies. Given the significant role of TROP2 in cell proliferation and transformation, as well as its overexpression in many epithelial solid tumors compared with normal tissue, several anti-TROP2 agents have entered clinical development. Specifically, several antibody–drug conjugates (ADC) have been designed to combine the targeting ability of mAbs with the cell-damaging effects of potent cytotoxic agents (19). In 2020, sacituzumab govitecan, an ADC targeting TROP2, became the first FDA-approved anti-TROP2 agent for the treatment of unresectable locally advanced or metastatic triple-negative breast cancer in patients refractory to previous systemic therapies (20). This drug is also now approved for patients with advanced metastatic hormone receptor (HR)-positive, HER2-negative breast cancer and advanced urothelial cancer.

Spira and colleagues reported the results of the NSCLC cohorts in the phase I TROPION-PanTumor01 trial, which investigated the safety and efficacy of another TROP2-directed ADC called datopotamab deruxtecan in patients with advanced solid tumors (21). One hundred seventy-five patients with advanced NSCLC were enrolled in the study. Eighty-four percent previously received immunotherapy, and 94% received platinum-based chemotherapy. Datopotamab deruxtecan demonstrated preliminary signals of activity with a manageable safety profile. More recently, the preliminary analysis of the TROPION-Lung02 trial, which investigated the combination of datopotamab deruxtecan and pembrolizumab in 47 patients with advanced NSCLC, revealed an objective response rate of 38% (95% CI, 25%–54%) and a median PFS of 10.8 months (95% CI, 8.3–15.2; ref. 22). Although these results were encouraging, our data suggest that a TROP2-biomarker-based strategy may be relevant in selecting patients with NSCLC who are more likely to benefit from a combination of immunotherapy and an anti-TROP2 agent. Given the observed correlation between TROP2 circulating levels, expression in tumor tissue, and patient outcomes, implementing a biomarker-driven strategy may also allow for noninvasive testing through a blood assay.

Ethical approval

This study was approved by the IRB of Institut Bergonié. All patients provided written informed consent.

Authors' Disclosures

A. Bessede reports other support from Explicyte during the conduct of the study. B. Besse reports grants from AbbVie, Amgen, AstraZeneca, Chugai Pharmaceutical, Daiichi-Sankyo, Ellipse Pharma, Eisai, Genmab, Genzyme Corporation, Hedera Dx, Inivata, Ipsen, Janssen, MSD, PharmaMar, Roche-Genentech, Sanofi, SOCAR Research, Tahio Oncology, and Turning during the conduct of the study. C. Rey reports other support from Explicyte during the conduct of the study. O. Lara reports other support from ImmuSmol during the conduct of the study. O. Odin reports other support from Exlicyte during the conduct of the study. F. Barlesi reports other support from AbbVie, ACEA, Amgen, AstraZeneca, Bayer, Bristol Myers Squibb, Boehringer Ingelheim, Eisai, Eli Lilly Oncology, F. Hoffmann–La Roche Ltd., Genentech, Ipsen, Ignyta, Innate Pharma, Loxo, Novartis, Medimmune, Merck, MSD, Pierre Fabre, Pfizer, Sanofi-Aventis, and Takeda outside the submitted work. J.P. Guégan is an employee of Explicyte. A. Italiano reports grants and personal fees from AstraZeneca, Bayer, Parthenon, and BMS; grants from MSD and Merck; personal fees from Lilly; and grants and personal fees from Transgene outside the submitted work. No disclosures were reported by the other authors.

Authors' Contributions

A. Bessede: Conceptualization, resources, supervision, funding acquisition, validation, investigation, methodology, writing–review and editing. **F. Peyraud:** Investigation, writing–review and editing. **B. Besse:** Investigation, writing–review and editing. **S. Cousin:** Investigation, writing–review and editing. **M. Cabart:** Investigation, writing–review and editing. **F. Chomy:** Investigation, writing–review and editing. **C. Rey:** Data curation, investigation, methodology, writing–review and editing. **O. Lara:** Validation, investigation, writing–review and editing. **O. Odin:** Validation, investigation, writing–review and editing. **I. Nafia:** Validation, investigation, writing–review and editing. **L. Vanhersecke:** Validation, investigation, writing–review and editing. **F. Barlesi:** Investigation, writing–review and editing. **J.-P. Guégan:** Data curation, formal analysis, validation, investigation, writing–original draft, writing–review and editing. **A. Italiano:** Conceptualization, resources, formal analysis, supervision, funding acquisition, writing–original draft, writing–review and editing.

Acknowledgments

Funding was provided by Conseil Regional Aquitaine (BIP AIRIC).

The publication costs of this article were defrayed in part by the payment of publication fees. Therefore, and solely to indicate this fact, this article is hereby marked "advertisement" in accordance with 18 USC section 1734.

Note

Supplementary data for this article are available at Clinical Cancer Research Online (http://clincancerres.aacrjournals.org/).

Received August 23, 2023; revised October 7, 2023; accepted November 29, 2023; published first December 4, 2023.

References

1. Shields MD, Marin-Acevedo JA, Pellini B. Immunotherapy for advanced non–small cell lung cancer: a decade of progress. Am Soc Clin Oncol Educ Book 2021;41:1–23.
2. Camidge DR, Doebele RC, Kerr KM. Comparing and contrasting predictive biomarkers for immunotherapy and targeted therapy of NSCLC. Nat Rev Clin Oncol 2019;16:341–55.

3. Cubas R, Zhang S, Li M, Chen C, Yao Q. Trop2 expression contributes to tumor pathogenesis by activating the ERK MAPK pathway. Mol Cancer 2010;9:253.
4. Guan H, Guo Z, Liang W, Li H, Wei G, Xu L, et al. Trop2 enhances invasion of thyroid cancer by inducing MMP2 through ERK and JNK pathways. BMC Cancer 2017;17:486.
5. Guerra E, Trerotola M, Tripaldi R, Aloisi AL, Simeone P, Sacchetti A, et al. Trop-2 induces tumor growth through AKT and determines sensitivity to AKT inhibitors. Clin Cancer Res 2016;22:4197–205.
6. Mito R, Matsubara E, Komohara Y, Shinchi Y, Sato K, Yoshii D, et al. Clinical impact of TROP2 in non–small lung cancers and its correlation with abnormal p53 nuclear accumulation. Pathol Int 2020;70:287–94.
7. Inamura K, Yokouchi Y, Kobayashi M, Ninomiya H, Sakakibara R, Subat S, et al. Association of tumor TROP2 expression with prognosis varies among lung cancer subtypes. Oncotarget 2017 Apr 25;8:28725–35.
8. Wang X, Long M, Dong K, Lin F, Weng Y, Ouyang Y, et al. Chemotherapy agents-induced immunoresistance in lung cancer cells could be reversed by trop-2 inhibition *in vitro* and *in vivo* by interaction with MAPK signaling pathway. Cancer Biol Ther 2013;14:1123–32.
9. Fehrenbacher L, Spira A, Ballinger M, Kowanetz M, Vansteenkiste J, Mazieres J, et al. Atezolizumab versus docetaxel for patients with previously treated non–small cell lung cancer (POPLAR): a multicenter, open-label, phase II randomized controlled trial. Lancet 2016;387:1837–46.
10. Rittmeyer A, Barlesi F, Waterkamp D, Park K, Ciardiello F, von Pawel J, et al. OAK Study Group. Atezolizumab versus docetaxel in patients with previously treated non–small cell lung cancer (OAK): a phase III, open-label, multicenter randomized controlled trial. Lancet 2017;389:255–65.
11. Eisenhauer EA, Therasse P, Bogaerts J, Schwartz LH, Sargent D, Ford R, et al. New response evaluation criteria in solid tumors: revised RECIST guideline (version 1.1). Eur J Cancer 2009;45:228–47.
12. Bindea G, Mlecnik B, Tosolini M, Kirilovsky A, Waldner M, Obenauf AC, et al. Spatiotemporal dynamics of intratumoral immune cells reveal the immune landscape in human cancer. Immunity 2013;39:782–95.
13. Hennequin A, Derangère V, Boidot R, Apetoh L, Vincent J, Orry D, et al. Tumor infiltration by Tbet+ effector T cells and $CD20^{+}$ B cells is associated with survival in gastric cancer patients. Oncoimmunology 2015;5:e1054598.
14. Massard C, Michiels S, Ferté C, Le Deley MC, Lacroix L, Hollebecque A, et al. High-throughput genomics and clinical outcome in hard-to-treat advanced cancers: results of the MOSCATO 01 trial. Cancer Discov 2017;7:586–95.
15. Filbin MR, Mehta A, Schneider AM, Kays KR, Guess JR, Gentili M, et al. Plasma proteomics reveals tissue-specific cell death and mediators of cell-cell interactions in severe COVID-19 patients. Biorxiv 2020.
16. Stoyanova T, Goldstein AS, Cai H, Drake JM, Huang J, Witte ON. Regulated proteolysis of Trop2 drives epithelial hyperplasia and stem cell self-renewal via β-catenin signaling. Genes Dev 2012;26:2271–85.
17. Guerra E, Trerotola M, Relli V, Lattanzio R, Tripaldi R, Vacca G, et al. Trop-2 induces ADAM10-mediated cleavage of E-cadherin and drives EMT-less metastasis in colon cancer. Neoplasia 2021;23:898–911.
18. Trabolsi A, Kareff SA, Rodriguez E, Krause HB, Tan H, Morgenstern-Kaplan D, et al. The genomic, transcriptomic, and immunological landscape of TROP2 in solid tumors. J Clin Oncol 2023;41:3118.
19. Parisi C, Mahjoubi L, Gazzah A, Barlesi F. TROP-2 directed antibody–drug conjugates (ADCs): The revolution of smart drug delivery in advanced non–small cell lung cancer (NSCLC). Cancer Treat Rev 2023;118:102572.
20. Bardia A, Mayer IA, Vahdat LT, Tolaney SM, Isakoff SJ, Diamond JR, et al. Sacituzumab govitecan-hziy in refractory metastatic triple-negative breast cancer. N Engl J Med 2019;380:741–51.
21. Spira A, Lisberg A, Sands J, Greenberg J, Philips P, Guevara F, et al. OA03.03 datopotamab deruxtecan (Dato-DXd; DS-1062), a TROP2 ADC, in patients with advanced NSCLC: updated results of TROPION-PanTumor01 phase I study. J Thorac Oncology 2021;3:S106–7.
22. Goto Y, Su WC, Levy BP, Rixe O, Yang TY, Tolcher AW, et al. TROPION-Lung02: Datopotamab deruxtecan (Dato-DXd) plus pembrolizumab (pembro) with or without platinum chemotherapy (Pt-CT) in advanced non–small cell lung cancer (aNSCLC). J Clin Oncol 2023;41:9004.